A Study of Impacts of Coupled Model Initial Shocks and State–Parameter Optimization on Climate Predictions Using a Simple Pycnocline Prediction Model

S. ZHANG

NOAA/GFDL, Princeton University, Princeton, New Jersey

ABSTRACT

A skillful decadal prediction that foretells varying regional climate conditions over seasonal–interannual to multidecadal time scales is of societal significance. However, predictions initialized from the climate-observing system tend to drift away from observed states toward the imperfect model climate because of the model biases arising from imperfect model equations, numeric schemes, and physical parameterizations, as well as the errors in the values of model parameters. Here, a simple coupled model that simulates the fundamental features of the real climate system and a "twin" experiment framework are designed to study the impact of initialization and parameter optimization on decadal predictions. One model simulation is treated as "truth" and sampled to produce "observations" that are assimilated into other simulations to produce observation-estimated states and parameters. The degree to which the model forecasts based on different estimates recover the truth is an assessment of the impact of coupled initial shocks and parameter optimization on climate predictions of interests. The results show that the coupled model initialization through coupled data assimilation in which all coupled model components are coherently adjusted by observations minimizes the initial coupling shocks that reduce the forecast errors on seasonal–interannual time scales. Model parameter optimization with observations effectively mitigates the model bias, thus constraining the model drift in long time-scale predictions. The coupled model state–parameter optimization greatly enhances the model predictability. While valid "atmospheric" forecasts are extended 5 times, the decadal predictability of the "deep ocean" is almost doubled. The coherence of optimized model parameters and states is critical to improve the long time-scale predictions.

1. Introduction

Because of the imperfect model structures such as model equations, numeric schemes, and physical parameterizations, as well as the errors in the values of model parameters, a coupled climate model is biased so that the model climate tends to drift away from the real world (Delworth et al. 2006; Collins et al. 2006). To obtain the initial conditions from which a model prediction can be started with the observed state, the measured data in the climate observing system are assimilated into a coupled model to estimate the historical and present climate states. However, due to the existence of model bias, the climate prediction initialized from the observing system also tends to drift away from the observed states toward the imperfect model climate (Smith et al. 2007).

Traditionally, one tries to mitigate the bias in initial conditions through a statistical method (e.g., Dee and Silva 1998; Dee 2005; Cherupin et al. 2005) or only assimilating (restoring) anomalies rather than the full values into a model (Smith et al. 2007; Keenlyside et al. 2008). Directly estimating model parameters using observations through expanding the adjustable variables of assimilation to include parameters is another approach to limit model bias (e.g., Anderson 2001; Annan and Hargreaves 2004; Annan et al. 2005; Aksoy et al. 2006a,b; Evensen 2007; Hansen and Penland 2007; Kondrashov et al. 2008; Tong and Xue 2008a,b; Yang and DelSole 2009; DelSole and Yang 2010). However, without modifying the traditional data assimilation procedure, effective parameter estimation is usually difficult within a coupled data assimilation (CDA) system in which multiple time scale model components are invloved, even though it is theoretically promising. In general, unlike traditional state estimation where the system states are directly adjusted by observations of states, without direct observations and prognostic equations, parameter estimation completely relies on the covariance between

Corresponding author address: Shaoqing Zhang, GFDL/NOAA, Princeton University, P.O. Box 308, Princeton, NJ 08542.
E-mail: shaoqing.zhang@noaa.gov

a parameter and the model state for projecting the observational information of state variables onto the parameter being estimated. The examination using a simple coupled model found that to establish a signal-dominant state–parameter covariance, the coupled model ensemble is required to be sufficiently constrained by observations that may come from different system components with different time scales, and otherwise the noisy covariance could bring the parameter toward an erroneous value (Zhang et al. 2011). This difficulty is relaxed by the proposed assimilation scheme with enhancive parameter correction. In that scheme, the signal-dominant covariance between a parameter and the model state facilitates parameter correction when coupled state estimation reaches a "quasi equilibrium" where the uncertainty of model states has been sufficiently constrained by observations and it therefore becomes more controlled by parameter errors. Once the observation-based parameter optimization is facilitated, numerical climate prediction based on a biased coupled model becomes a "coupled state–parameter optimization problem" rather than only a "state initial value problem." How much of the model drift in decadal predictions can be constrained by the coupled model state–parameter optimization? A simple pycnocline prediction model that characterizes the seasonal–interannual (SI) to decadal variability of the climate system and a "twin" experiment framework are designed to address this question. In the twin experiment framework, one model simulation is treated as "truth" and is sampled to produce "observations," and then the synthetic "observations" are assimilated into other simulations to produce observation-optimized model states or observation-optimized model states and parameters. The degree to which the model forecasts based on different assimilation results recover the truth is used to assess the impact of different coupled initialization schemes as well as observation-optimized model parameters on climate predictions.

The motivation of this study is mainly to present the impacts of minimized initial coupling shocks in coupled data assimilation on climate predictions with various time scales, and as the whole topic of climate predictability enhancement, they are linked with the impact of coupled model state-parameter optimization. Although some of the preliminary results on the impact of observation-optimized model parameters on decadal prediction from this study have been briefly reported in a letter (Zhang 2011), here the author still presents the details of the impact of coupled model state–parameter optimization with observations on various time-scale climate predictions. After describing the construction of the simple pycnocline prediction model, section 2 first gives a brief description for the ensemble filter and then presents the

design of the twin experiment framework, both of which will be used throughout the paper for state estimation and parameter optimization, as well as the prediction assessment. In the twin experiment framework, an assimilation model is set with a set of erroneous values for all model parameters while the "truth" model with a set of "standard" parameter values defines the "true" solution for the estimation and prediction problem, and the observations are samples of the true solution. Section 3 examines the impact of minimized initial shocks on various time-scale climate predictions using the coupled data assimilation procedure. Section 4 examines the impact of the coupled model state–parameter optimization on long time-scale climate predictions. Conclusions and discussions are given in section 5.

2. Methodology

a. A simple pycnocline prediction model

Because of the complex physical processes and huge computational cost involved, it is not convenient to use a coupled general circulation model (CGCM) to clearly address the impact of coupled model initial shocks and state-parameter optimization on climate predictions. Instead, as the first step of the studies on this research topic, the author constructs a simple decadal prediction model in this section. For the problem that is concerned, this simple decadal prediction model shall share the following fundamental features of a CGCM:

1) the ocean variability is a consequence of the response of the slow ocean to the fast atmosphere, and in return the air–sea interaction can modify the statistical character of the atmosphere;

2) while much slower deep ocean is driven by the upper ocean, as the feedback it also modulates low-frequency variability of the upper ocean so as to impact on the atmosphere through the air-sea interaction; and

3) a perturbation on any parameter of each model component can change the model solution.

The construction starts from the simple coupled model developed in the previous study (Zhang et al. 2011) in which a slowly-varying variable w is coupled with the Lorenz's 3-variable chaotic model (Lorenz 1963) to simulate the interaction of the fast atmosphere with the slow upper ocean:

$$\dot{x}_1 = -\sigma x_1 + \sigma x_2$$
$$\dot{x}_2 = -x_1 x_3 + (1 + c_1 w)\kappa x_1 - x_2$$
$$\dot{x}_3 = x_1 x_2 - b x_3$$
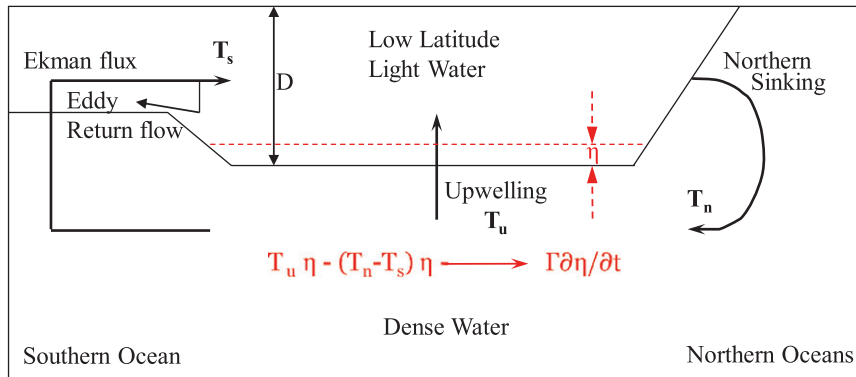$$O_m \dot{w} = c_2 x_2 - O_d w + S_m + S_s \cos(2\pi t/S_{pd}), \quad (1)$$

FIG. 1. The linear response of pycnocline anomaly (η) to the residual of the low-latitude upwelling and the net transport between the Northern Hemisphere sinking minus the northward Ekman flux in the Southern Ocean serving as the leading-order term of the time tendency of η (red), based on Gnanadesikan's balance model for the zonal mean pycnocline depth (Gnanadesikan 1999) (black).

where an overdot denotes time tendency; x_1, x_2, and x_3 are the high-frequency variables of the atmosphere with the original σ, κ, and b parameters and their standard values 9.95, 28, and 8/3, which sustain the chaotic nature of the atmosphere. For w, except for a forcing term from the atmosphere ($c_2 x_2$), the simplest slab ocean only consists of a linear damping term $-O_d w$ and an imposed external forcing. An important feature of w is that it must have a much slower time scale than the atmosphere, which can be obtained by requiring a much larger heat capacity than the damping rate, that is, $O_m \gg O_d$. For example, the values of (10, 1) for (O_m, O_d) define the oceanic time scale as $\sim O(10)$, 10 times of the atmospheric time scale $\sim O(1)$. Also simply setting the external forcing as $S_m + S_s \cos(2\pi t/S_{pd})$ simulates the constant and seasonal forcings for the "climate" system so that the "ocean" is recharged when it is damped, where S_{pd} defines the period of seasonal cycle. The S_{pd} is chosen as 10 so that the period of the forcing is comparable with the oceanic time scale, defining the time scale of the model seasonal cycle. The parameters S_m and S_s define the magnitudes of the annual mean and seasonal cycle of the forcings, which are not sensitive to the model construction and set as 10 and 1, respectively. The coupling between the fast atmosphere and slow ocean is realized by choosing the values of the coupling coefficients c_1 and c_2, with c_1 representing the oceanic forcing on the atmosphere, and c_2 representing the atmospheric forcing on the ocean. Here, the multiplicative way of ocean to force the atmosphere allows the coupling forcing to produce some modulation for the atmospheric attractor, and for simplicity, only one oceanic forcing as a multiplicative forcing is kept in the x_2 equation. Experiments show that the coupled system is robust with respect to c_2 but becomes unstable when c_1 is much larger than 0.1, so c_1 and c_2 are set as 0.1 and 1, respectively. A set of

standard parameter values (σ, κ, b, c_1, c_2, O_m, O_d, S_m, S_s, S_{pd}) = (9.95, 28, 8/3, 10^{-1}, 1, 1, 10, 10, 1, 10) was used to simulate the fundamental character of the coupled climate system in tropics. Forced by the fluxes of the "chaotic" atmosphere, the slow ocean w generates its internal "seasonal–interannual" variability with a 10-times larger time scale than that of the atmospheric variables $x_{1,2,3}$ [usually about 1 nondimensional time unit (TU)]. Moreover, the forcing from the ocean to the atmosphere alters the centers of the lobe of the atmospheric attractor.

The other important component of the simple decadal prediction model is a simple pycnocline predictive model derived from the two-term balance model of the zonal–time mean pycnocline (Gnanadesikan 1999). Gnanadesikan described how the low-latitude upwelling heat flux ($T_u D$) balances the net transport of the Northern Hemisphere (NH) sinking minus the northward Ekman flux in the Southern Ocean (SO) [($T_n - T_s$)D], to maintain the zonal–time mean pycnocline depth D (illustrated by the black background in Fig. 1). Fluctuations of the pycnocline depth (η) occur when the low-latitude upwelling cannot be completely compensated by the net transport between the NH sinking and the SO Ekman flux (denoted by red symbols in Fig. 1). Assuming that the leading-order time tendency of the anomalous pycnocline ($\partial\eta/\partial t$) is a linear response to the residual between $T_u\eta$ and ($T_n - T_s$)η, the linear prediction equation of η is $\Gamma\partial\eta/\partial t = T_u\eta - (T_n - T_s)\eta$, where Γ is a constant of proportionality. Here, $T_u\eta$ can be approximated by the total vertical diffusion in the low-latitude box (Gnanadesikan 1999), which can also be assumed as a linear term of the slab ocean variable w, that is, cw, and ($T_n - T_s$)η can be simplified as $r\eta$, with c and r being a simple constant of proportionality. The basic linear equation that conceptually describes the time evolution of the deep ocean
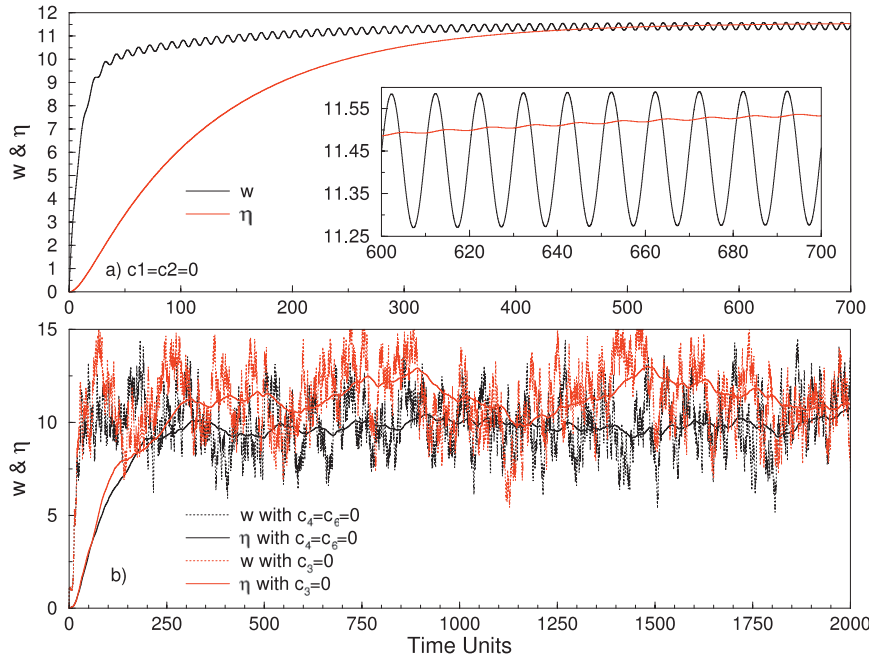
FIG. 2. Time series of the upper-ocean variable w and the deep ocean pycnocline depth anomaly η (a) without the interaction of atmosphere and ocean [i.e., $c_1 = c_2 = 0$ in Eq. (2)] (black for w and red for η) and (b) with the interaction of atmosphere and ocean but only the linear interaction of η to w (i.e., setting $c_4 = c_6 = 0$) (black-dashed for w and black-solid for η) or only the nonlinear interaction of w and η (i.e., setting $c_3 = 0$) (red-dashed for w and red-solid for η) remaining. The section of 600–700 TUs of (a) is zoomed out to show the damped oscillations of η compared to the w's when the ocean does not have the stochastic atmospheric forcings.

pycnocline becomes $\Gamma \partial \eta / \partial t = cw - r\eta$. The term $-r\eta$ also represents the damping mechanism, and for this simple system, only accounting for the ocean's viscosity, we set $r = O_d$ where O_d is the damping coefficient of the slab ocean variable w. The ratio of Γ and O_d determines the time scale of variations of η, for example, a value of 100 for Γ defining 10 "seasonal" cycles of w (a model decade) as the typical time scale of η variability. To simulate the effects of the nonlinear advection in the upper and deep oceans, the nonlinear terms are introduced into w and η equations. Finally, the conceptual pycnocline prediction model takes the form as

$$\dot{x}_1 = -\sigma x_1 + \sigma x_2$$
$$\dot{x}_2 = -x_1 x_3 + (1 + c_1 w)\kappa x_1 - x_2$$
$$\dot{x}_3 = x_1 x_2 - b x_3$$
$$O_m \; \dot{w} = c_2 x_2 + c_3 \eta + c_4 w\eta - O_d w + S_m$$
$$+ \, S_s \cos(2\pi t / S_{\text{pd}})$$
$$\Gamma \; \dot{\eta} = c_5 w + c_6 w\eta - O_d \eta, \qquad (2)$$

which includes 5 model variables (x_1, x_2, and x_3 for the atmosphere, w for the slab ocean, and η for the deep

ocean pycnocline) and 5 new parameters. For the equation of w, c_3 and c_4 represent the linear forcing of the deep ocean and the nonlinear interaction of the upper and deep oceans, and we set their magnitude order smaller than that of c_2 [note $c_2 \sim O(1)$] to retain the leading-order role of the atmosphere–ocean coupling for the slab ocean. For η, we set $c_5 \sim O(1)$ to retain the leading-order role of the linear response of the deep ocean to the upper ocean. Also assuming that the nonlinearity of the deep ocean is weaker than that of the upper ocean, the order of c_6 is set smaller than that of c_4. Given these constraints, experiments show that the model construction is robust and not quite sensitive to the values of these coefficients, and we choose c_3 and $c_4 \sim O(10^{-2})$ and $c_6 \sim O(10^{-3})$.

Using a leapfrog time differencing scheme ($\Delta t = 0.01$) with a Robert–Asselin time filter (Robert 1969; Asselin 1972) (denote the time filtering coefficient as $\gamma = 0.25$), the model is first spun up for 10^4 TUs starting from (x_1, x_2, x_3, w, η) = (0, 1, 0, 0, 0) with the values of 16 model parameters described above, that is, (σ, κ, b, c_1, c_2, O_m, O_d, S_m, S_s, S_{pd}, Γ, c_3, c_4, c_5, c_6, γ) = (9.95, 28, 8/3, 10^{-1}, 1, 1, 10, 10, 1, 10, 100, 10^{-2}, 10^{-2}, 1, 10^{-3}, 0.25). Figure 2a first shows that without the stochastic atmospheric forcings, the upper ocean w is a simple seasonal oscillation defined
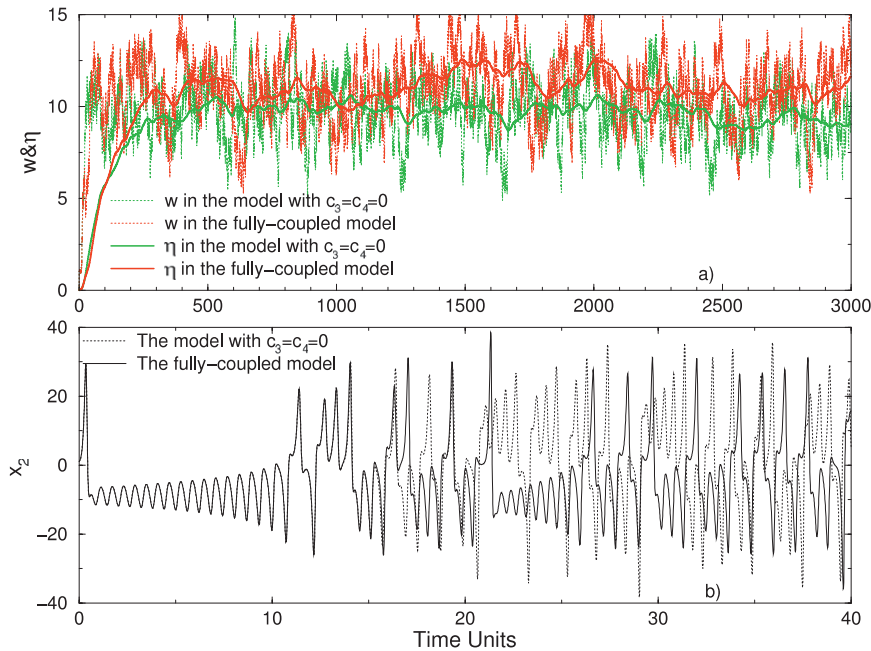
FIG. 3. Time series of (a) the upper-ocean variable w (dotted) and the deep ocean pycnocline depth anomaly η (solid) and (b) the atmospheric variable x_2 produced by Eq. (2) starting from the initial conditions $(x_1, x_2, x_3, w, \eta) = (0, 1, 0, 0, 0)$. The dotted (solid) green lines in (a) [for w (η)] and the dotted black line in (b) (for x_2) are the results of the model without the upper-ocean and deep ocean coupling [i.e., setting $c_3 = c_4 = 0$ in Eq. (2), which degrades to the upper ocean and atmosphere coupled model described by Eq. (1)]. The solid-green line in (a) is the result of integrating the η equation that only depends on the w values from the upper ocean and atmosphere coupled model without any feedback of η to w.

by S_{pd}, and the deep ocean η is a damped oscillation based on the input of w. With the atmospheric forcings, the model then is run only with the linear interaction of w and η (i.e., setting $c_4 = c_6 = 0$) or only with the nonlinear interaction of w and η (i.e., setting $c_3 = 0$), and results are shown in Fig. 2b. From Fig. 2b, it is clear that the linear terms in the w and η equations respond to the atmospheric forcings to create interannual to decadal scale oscillations for the deep ocean, while the nonlinear terms tend to modulate longer time scale variability.

An interesting aspect of the model is the influence of the η–w interaction on the upper ocean and atmosphere. Figs. 3 and 4 show the variability of the ocean and atmosphere with or without the feedback of η on the upper ocean by setting c_3 and c_4 as 10^{-2} or 0 (Fig. 3) as well as the corresponding power spectrum (Fig. 4). It is clear that the feedback of η to w helps transfer the energy of deep ocean from the subdecadal scales to decadal and interdecadal scales. The model variability shows that the upper ocean includes high-frequency and low-frequency variability, and the upper ocean can be transient by the more slowly varying deep ocean so that the deep ocean has an impact on the atmosphere attractor through the air–sea interaction. Namely, the simple model simulates the

fundamental features of the real world climate system— the upper ocean interacts with the transient atmospheric attractor above and the deep ocean below—the decadal and longer time scale variability of deep ocean has the impact on the transient atmospheric attractor through the feedbacks of the upper ocean to the atmosphere.

b. Coupled data assimilation with an ensemble filter for state and parameter estimations

An ensemble filter uses the error statistics evaluated from ensemble model integrations, such as error covariances between model states, to extract observational information to adjust the model ensemble for state estimation (e.g., Evensen 1994; Anderson 2001; Hamill et al. 2001). The ensemble-evaluated covariances between model states and model parameters can also be used to estimate the model parameters (e.g., Anderson 2001; Annan and Hargreaves 2004; Annan et al. 2005; Aksoy et al. 2006a,b; Evensen 2007; Hansen and Penland 2007; Kondrashov et al. 2008; Tong and Xue 2008b; Yang and DelSole 2009; DelSole and Yang 2010). Based on the two-step ensemble adjustment Kalman filter (EAKF; Anderson 2001; 2003; Zhang and Anderson 2003; Zhang et al. 2007), once the ensemble observation increment is computed [see Eqs.
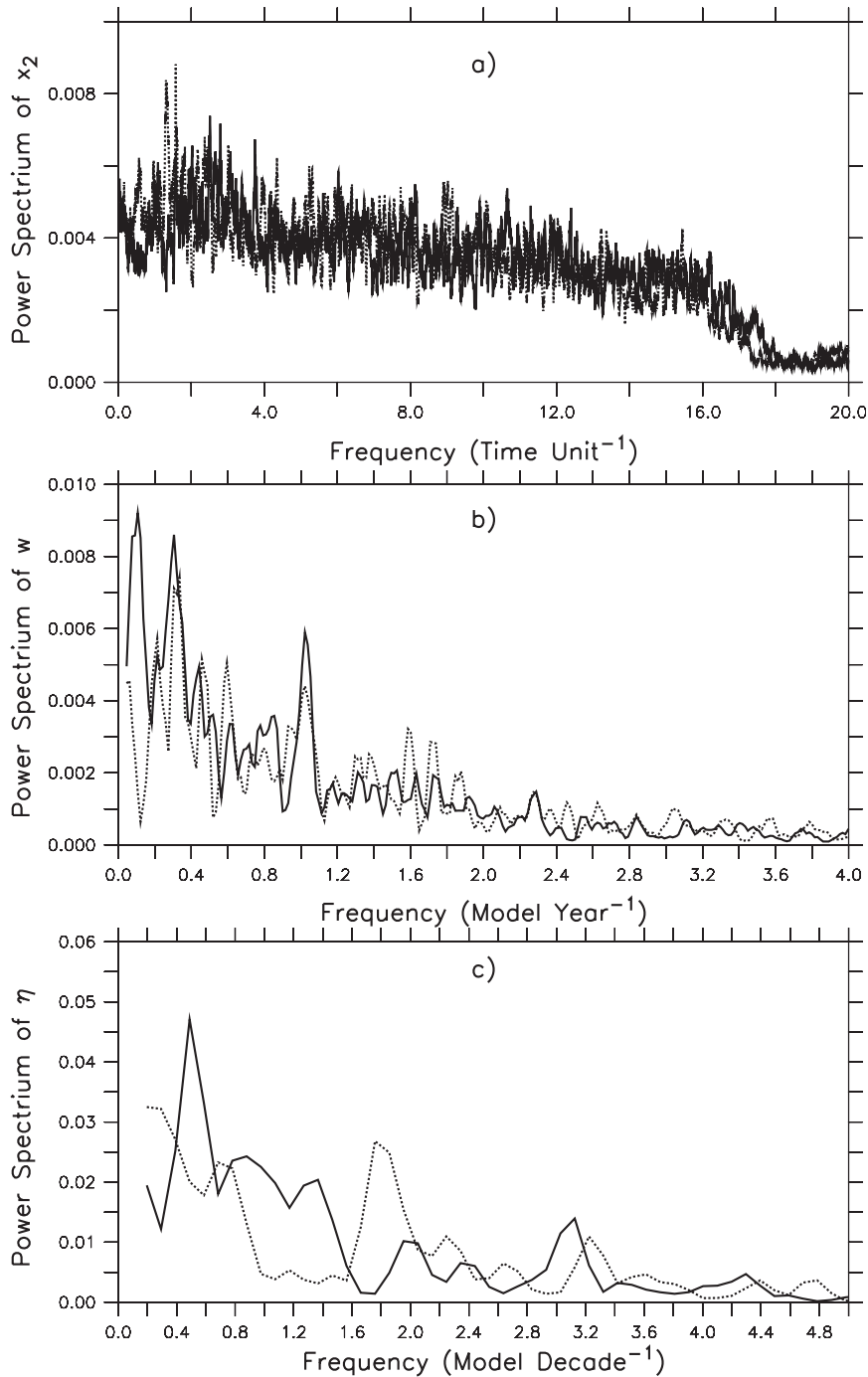
FIG. 4. The power spectrum of (a) x_2, (b) w, and (c) η based on the model data of 10^4-TU integrations after the spinup shown in Fig. 3. The dotted lines are for the model without the feedback of the deep ocean η to the upper ocean w [setting $c_3 = c_4 = 0$ in Eq. (2)].

(1)–(5) of Zhang et al. 2007], the filtering process can be expressed as a linear regression equation:

$$\Delta z_{j,i}^u = \frac{c(\Delta \mathbf{z}_j^p, \Delta \mathbf{y}_k)}{\sigma_k^2} \Delta y_{k,i}^o, \qquad (3)$$

where $\Delta y_{k,i}^o$ is the observational increment at the kth observational location for the ith ensemble member, $c(\Delta \mathbf{z}_j^p, \Delta \mathbf{y}_k)$ is the error covariance computed from the prior ensemble of the jth model variable or parameter and the model-estimated observation ensemble at location
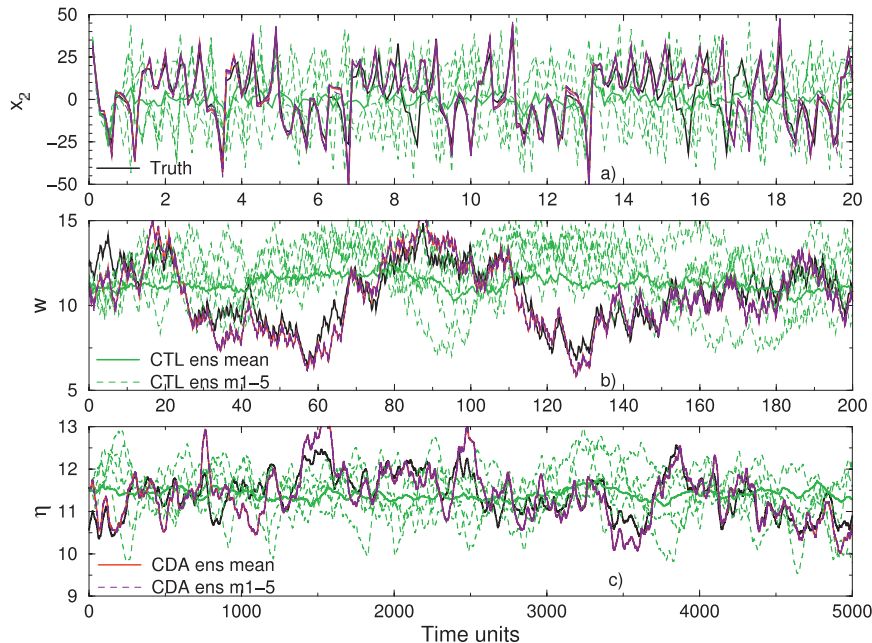
FIG. 5. Time series of the ensemble mean (solid) and the first five ensemble members (dashed) of (a) x_2, (b) w, and (c) η produced by the free model ensemble control (CTL) (green) of the assimilation model in which all 16 parameters have been overestimated by 10% from the standard values that are used to produce the truth (black), and the coupled data assimilation (red) by incorporating the atmospheric and oceanic observations (see section 2c) into the coupled model.

k, and σ_k is the standard deviation of the model ensemble at location k. the quantity $\Delta z_{j,i}$ is the adjustment amount for the jth model variable or parameter of the ith ensemble member.

The application of Eq. (3) to the state variables (replacing $\mathbf{z}_j$ by the state vector $\mathbf{x}_j$ with j as the index of model state variables) of a coupled model when reliable observations are available implements CDA for state estimation in a straightforward manner (Zhang et al. 2007). However, effective parameter estimation is usually difficult before the uncertainty of model states in CDA has been sufficiently constrained by observations. To have an enhancive parameter correction with observational information, the application of Eq. (3) for coupled parameter estimation (replacing $\mathbf{z}_j$ by the parameter ensemble vector β_l with l as the index of model parameters) has to be delayed until the state estimation reaches a quasi-equilibrium, where the errors of model states become mainly contributed from model parameter errors. With the modified data assimilation scheme, coupled data assimilation with parameter optimization (CDA$_{PO}$) is facilitated using the covariance between a parameter and the model state when the state estimation of CDA reaches quasi equilibrium. More discussion about the application of the CDA$_{PO}$ scheme to the simple pycnocline

prediction model developed in section 2a will be given in section 4, where the impact of observation-optimized parameters on decadal-scale climate predictions is addressed through twin experiments described below.

c. Twin experiment setup

The decadal prediction model with the standard parameter values described in section 2a produces the true solution for the assimilation–prediction problem, called truth. The observations are samples of the truth model states after the spinup of 10^4 TUs. A random noise is superimposed on the values of $x_{1,2,3}$ and w at an interval of 0.1 and 0.4 TU, respectively. The observational frequency simulates the feature of the real climate observing system in which the atmospheric observations are available more frequently (subdaily) than the oceanic observations (roughly-daily). Also, to simulate the lack of deep ocean measurements in the real observing system, no observation is available for η. The standard deviation of observational errors is 2 for $x_{1,2,3}$ and 0.5 for w. A biased assimilation–prediction model in which all parameters are set to have a 10% overestimated error from their standard values is used to assimilate the observations into the model and predict the truth by traditional CDA or CDA$_{PO}$ schemes. As the truth model does, starting

TABLE 1. List of model simulations (2), data assimilation experiments (2), and forecast experiments (8) used to study the impacts of coupled model initial shocks and state–parameter optimization with observations.

Abbreviation	Description	Values of parameters	Initial conditions
Truth	Model simulation	Standard values set in section 2a	Spun-up states with standard parameter values
CTL	Model simulation	Erroneous values set in section 2c	Spun-up states with erroneous parameter values
CDA	Coupled data assimilation	erroneous values set in section 2c	Spun-up states with erroneous parameter values
CDA_{PO}	Coupled data assimilation with parameter optimization	Initially from erroneous values but optimized by observations	Spun-up states with erroneous parameter values
$F^{Atm(CTL)}_{Ocn(CTL)}$	Model forecast initialized from CTL	Erroneous values set in section 2c	Taken from CTL
$F^{Atm(CTL)}_{Ocn(Truth)}$	Model forecast initialized from CTL & Truth	”	Atm taken from CTL and Ocn taken from Truth
$F^{Atm(Truth)}_{Ocn(CTL)}$	Model forecast initialized from CTL & Truth	”	Atm taken from Truth and Ocn taken from CTL
$F^{Atm(CDA)}_{Ocn(CDA)}$	Model forecast initialized from CDA	”	Taken from CDA
$F^{P(CDA_{PO})}_{ICs(CDA_{PO})}$	Model forecast initialized from CDA_{PO}	Observations-optimized values	Taken from CDA_{PO}
$F^{P(Truth)}_{ICs(CDA_{PO})}$	”	Standard values set in section 2a	Taken from CDA_{PO}
$F^{P(CDA_{PO})}_{ICs(Truth)}$	Model forecast initialized from Truth	Observation-optimized values	Taken from Truth
$F^{P(CDA_{PO})}_{ICs(CDA)}$	Model forecast initialized from CDA	”	Taken from CDA

from the initial conditions $(0, 1, 0, 0, 0)$, the assimilation model is also spun up for 10^4 TUs, which shows entirely different variability (green lines in Fig. 5) from the truth (black lines in Fig. 5). A Gaussian white noise with the same standard deviation as observational errors is added on the model state at the end of spinup to form the ensemble initial conditions from which the ensemble filtering data assimilation starts.

The synthetic observations produced by the truth model are assimilated into the assimilation model by the ensemble filter described in section 2b through CDA to estimate model states only or CDA_{PO} to optimize both model states and parameters. The ensemble size is chosen as 20 from a series of sensitivity tests based on the trade-off between the cost and assimilation quality (Zhang and Anderson 2003) and consistent with the leapfrog time differencing, a two-time-level adjustment scheme (Zhang et al. 2004) is employed in all data assimilation experiments in this study. The degree to which the predictions initialized from the CDA-estimated model states or CDA_{PO}-optimized model states and parameters recover the truth is an assessment of the impact of the coupled model state–parameter optimization on the predictions of interests. In this twin experiment framework, all estimated and forecasted fields are verified with the truth and the error statistics as the anomaly correlation coefficient (ACC) and the root-mean-square (RMS) error are used to measure the skills of assimilation and prediction. Beside the truth model simulation, a free model control simulation (without any observational constraint),

in which the assimilation model starts from the assimilation initial conditions described above, is conducted (briefly denoted as CTL) to establish a reference for evaluation of data assimilation effects. Therefore in this study, there are two model simulations, two data assimilation experiments, and a series of forecast experiments (totally eight), which are used to detect the impacts of coupled model initial shocks and state–parameter optimization with observations, for which the detailed description is summarized in Table 1.

3. Impact of minimized initial shocks on ensemble climate predictions through coupled data assimilation

To assess the influences of initial shocks on climate predictions using different coupled initialization schemes, we first conduct the fully coupled data assimilation to produce the time series of observation-estimated states of the coupled model. The CDA simultaneously incorporates the "atmospheric observations" (every 0.1 TU) and "oceanic observations" (every 0.4 TU) into the coupled model ensemble. Similar to the CGCM cases (e.g., Zhang et al. 2007, 2009; Zhang and Rosati 2010), considering entirely different time scales between the deep ocean and the atmosphere, we limit the impact of the atmospheric observations only on the atmosphere ($x_{1,2,3}$) and the upper ocean (w) while the oceanic observations (w) impact all variables of the atmosphere and ocean. Although an adaptive inflation algorithm (Anderson 2007)

TABLE 2. The RMS errors and ACCs of the atmospheric and oceanic variables in CDA and CDA$_{PO}$ as well as a free model control ensemble simulation (CTL).

Expt	Rms					ACC				
	Atm			Ocn		Atm			Ocn	
	x_1	x_2	x_3	w	η	x_1	x_2	x_3	w	η
CTL	152	242	313	3.1	0.38	—	—	—	—	—
CDA	52	130	170	1.2	0.10	0.84	0.78	0.77	0.87	0.91
CDA$_{PO}$	0.44	1.3	1.5	0.16	0.03	1	1	1	1	1

is available for a sophisticated system, for this simple system, a best-tuned inflation coefficient of 1.12 is applied to the prior ensemble of the atmosphere and upper-ocean variables. The CDA reconstructs the truth variability of the atmosphere and ocean mostly as shown in Fig. 5, quantified by the high ACC values (0.8 for the atmosphere and 0.89 for the ocean) and the significantly reduced RMS errors (by 47% for the atmosphere'' and by 63% for the ocean) compared to the free model control without initialization (CTL) (Table 2). The results here show that different from a filter with an unbiased assimilation model where the assimilation error can be expected smaller than the observational error by tuning the filtering inflation, a filter with a biased coupled model in which some component with large time-scale variability lacks observations may not well converge by tuning the filtering inflation. Section 4 will show that under this circumstance, while the model states are constrained by observations, properly optimizing the model parameters using observations is particularly important to make the filter convergent.

Next, we use the notation F with a subscript that represents the oceanic initial conditions and a superscript for atmospheric initial conditions, so that $F_{\text{Ocn(CDA)}}^{\text{Atm(CDA)}}$ stands for the forecast experiment in which both the atmosphere and the ocean of the coupled model are initialized from the CDA-estimated states. Beside $F_{\text{Ocn(CDA)}}^{\text{Atm(CDA)}}$ another two forecast experiments $F_{\text{Ocn(CTL)}}^{\text{Atm(Truth)}}$ and $F_{\text{Ocn(Truth)}}^{\text{Atm(CTL)}}$ also are used for assessing the impact of minimized initial shocks of CDA on climate predictions. In $F_{\text{Ocn(CTL)}}^{\text{Atm(Truth)}}$ ($F_{\text{Ocn(Truth)}}^{\text{Atm(CTL)}}$), the model ensemble is initialized from the perfect atmosphere (ocean) taken from the truth combined with the CTL oceanic (atmospheric) ensemble as shown by the dashed-green lines in Fig. 5. Another forecast experiment in which both the atmosphere and the ocean are initialized from the CTL ensemble coupled states, called $F_{\text{Ocn(CTL)}}^{\text{Atm(CTL)}}$, is used as a reference to establish the value of the initialization for the coupled model prediction. The detailed description of all the forecast experiments performed in this study can be found in Table 1. For each experiment, we launch 50 forecasts, each with a lead time of 500 TUs. The initial conditions are taken every 500 TUs apart over the period of 10^4 to 4×10^4 TUs. Figures 6

and 7 show some examples of the forecasted atmospheric (Fig. 6) and oceanic (Fig. 7) states produced by $F_{\text{Ocn(CDA)}}^{\text{Atm(CTL)}}$ (left columns) and $F_{\text{Ocn(Truth)}}^{\text{Atm(CTL)}}$ (right columns), while Fig. 8 shows the variation of the forecasted ACCs of the upper-ocean variable w with the forecast lead times.

Generally, compared to the coherent initial conditions of $F_{\text{Ocn(CDA)}}^{\text{Atm(CDA)}}$ (Figs. 6a,c and Figs. 7a,c), an inconsistency exists between x_2 and w in the initial conditions of $F_{\text{Ocn(CTL)}}^{\text{Atm(Truth)}}$ and $F_{\text{Ocn(Truth)}}^{\text{Atm(CTL)}}$ (only the $F_{\text{Ocn(Truth)}}^{\text{Atm(CTL)}}$ case is shown). While the imbalance caused by the inconsistency produces a zig-zag variation for the w (Figs. 7b,d), due to the strong internal variability of the atmosphere, the computational variability of the atmosphere caused by the imbalance is formed very rapidly (Figs. 6b,d). Specifically, in this simple system, the computational oscillations of x_2 caused by the imbalance between the atmospheric and oceanic initial conditions increase the "noises" of the "atmospheric" forcings to w. These increased errors on the "atmospheric" fluxes to the "ocean" produce a larger decreasing rate of the forecast ACC of w with the forecast lead times in $F_{\text{Ocn(Truth)}}^{\text{Atm(CTL)}}$ than in $F_{\text{Ocn(CDA)}}^{\text{Atm(CDA)}}$ (Fig. 8), resulting lesser forecast skills of $F_{\text{Ocn(Truth)}}^{\text{Atm(CTL)}}$ after 1.5-TU forecasts even though it starts from the perfect oceanic initial conditions.

It is worth mentioning that due to the marginal impact of the upper ocean on the deep ocean in this simple model (as shown in Fig. 3a), the initial shocks induced by the imbalance between x_2 and w in the initial conditions of $F_{\text{Ocn(CTL)}}^{\text{Atm(Truth)}}$ and $F_{\text{Ocn(Truth)}}^{\text{Atm(CTL)}}$ do not explicitly influence on the forecast skills of the deep ocean adversely.

4. Impact of the coupled model state–parameter optimization on climate predictions

The results of section 3 show that when a filter is applied to a biased coupled model in which some component with large time-scale variability lacks observations, it is difficult to make the filter convergent through tuning the filtering inflation. In this section, the author will show that under such a circumstance, properly optimizing model parameters using observations is an effective approach to enhance the accuracy of state estimation and improve model predictions.

a. Model sensitivities on parameters

The sensitivity study of a model on parameters is an important step to understand the role of each parameter in the model and implement parameter estimation (e.g., Tong and Xue 2008a,b). In particular, the sensitivity of a model to a parameter is a key to determine the inflation of the prior ensemble of the parameter, which is an indispensable part of ensemble-based parameter estimation (e.g., Annan and Hargreaves 2004; Annan et al. 2005;
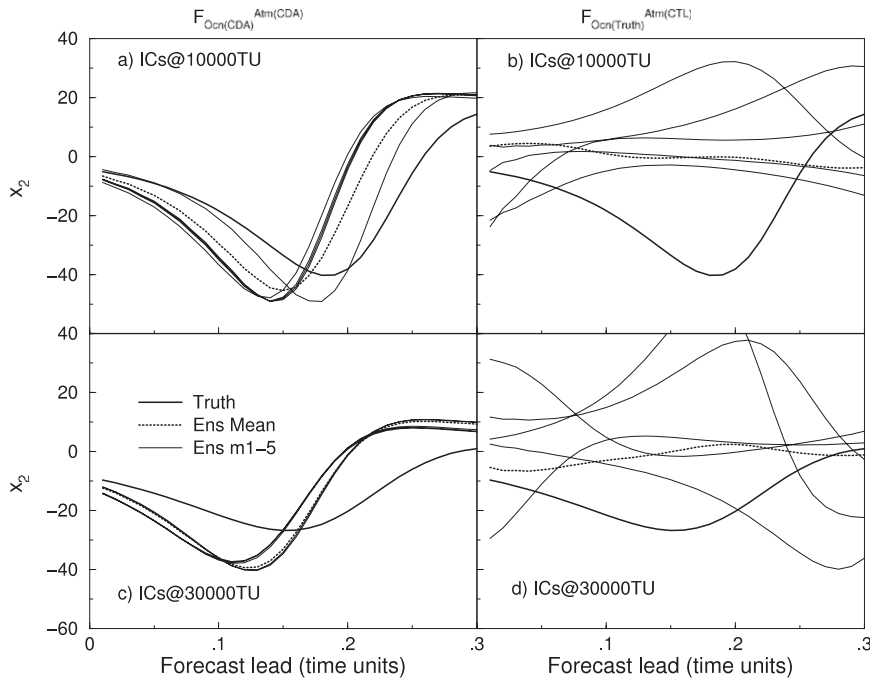
FIG. 6. Time series of x_2 in (a),(c) $F_{Ocn(CDA)}^{Atm(CDA)}$ and (b),(d) $F_{Ocn(Truth)}^{Atm(CTL)}$ as the model is initialized at the (a),(b) 10 000th and (c),(d) 30 000th time unit. The experiment $F_{Ocn(CDA)}^{Atm(CDA)}$ uses the coupled model ensemble states produced by the coupled data assimilation described in section 3 as initial conditions, while the forecasts of $F_{Ocn(Truth)}^{Atm(CTL)}$ are initialized from the CTL atmospheric ensemble combined with the perfect oceanic states taken from the truth.

Aksoy et al. 2006ab; Evensen 2007). Here, the model sensitivity to each parameter is assessed by examining the temporal evolution of the ensemble standard deviation of model states when the examined parameter is perturbed with a Gaussian white noise on its default value at the initial time. To do so, the model ensemble is iteratively integrated for each parameter that is perturbed by the Gaussian random noise with the default
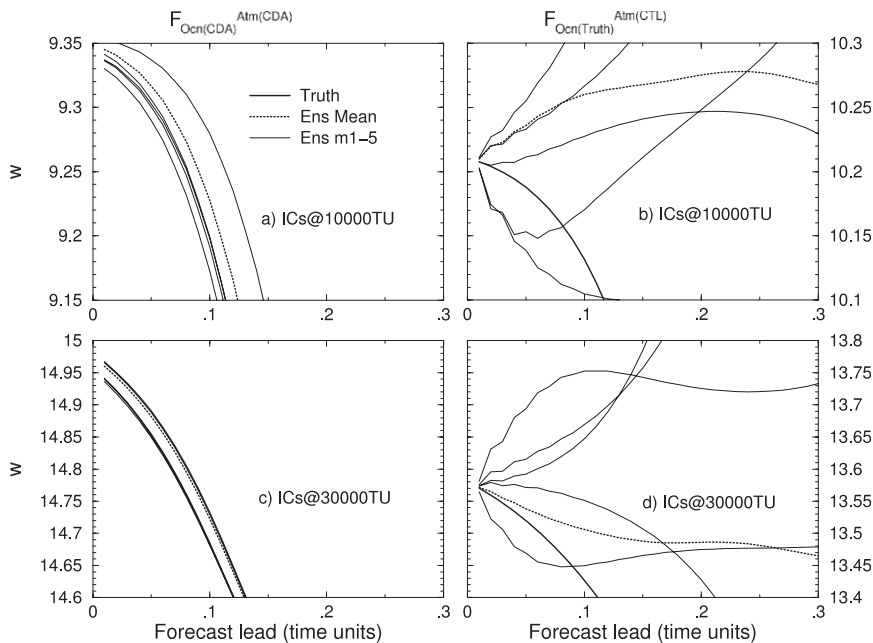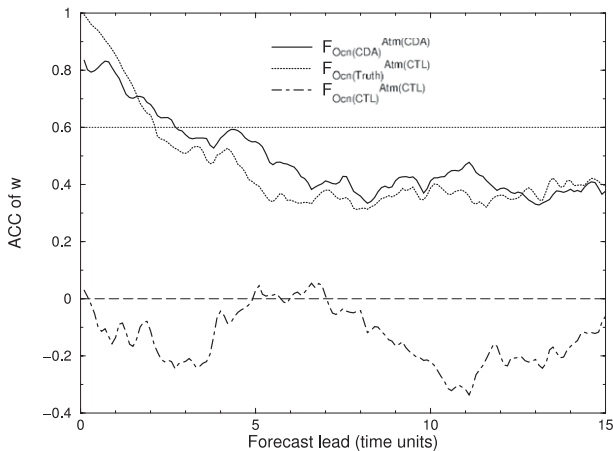

FIG. 7. As in Fig. 6, but for w.

FIG. 8. Variations of the ACCs of w with the forecast lead time, produced by the $F_{\text{Ocn(CDA)}}^{\text{Atm(CDA)}}$ (solid), $F_{\text{Ocn(Truth)}}^{\text{Atm(CTL)}}$ (dotted), and $F_{\text{Ocn(CTL)}}^{\text{Atm(CTL)}}$ (dashed) forecast experiments. The dotted- (dashed-) gray line marks the 0.6 (0) ACC value.

FIG. 9. (a) Time series of standard deviations of the ensemble of η when a model parameter is perturbed by a Gaussian noise with the standard deviation as 5% of its default value for the cases of σ (solid), O_d (dotted), S_m (dashed), and c_5 (dotted-dashed); (b) averaged standard deviations of the ensemble of η over 500–1000 TUs when the model parameter being examined is perturbed by the Gaussian noise for each of the 16 parameters, referred as to σ_l, $l = 1, 16$.

value (described in section 2c) as the mean and 5% of the default value as the standard deviation. The model ensemble for each parameter is integrated for 2000 TUs starting from the intial conditions created by the spinup described in section 2c.

Generally, while the model shows an almost instant sensitivity to the atmospheric parameters (within a TU) and a slow response on the perturbation of oceanic parameters (2–10 TUs), the ensemble spreads of the atmospheric variables and the upper-ocean variable w do not show a significant difference for different parameters after 10 TUs of model integrations. Interestingly the deep ocean variable η shows different sensitivities to parameters. We will use the η sensitivities to implement parameter optimization to target the "decadal" variability of this model. As examples, the time series of the standard deviations of the ensemble of η for the cases that σ, O_d, S_m, and c_5 are perturbed by the Gaussian noise are shown in Fig. 9a. The averaged η spread with respect to each parameter (referred as σ_l for the lth parameter) over 500–1000 TUs are shown in Fig. 9b as the measurement of the model sensitivity with respect to each parameter, which will be used to determine the inflation coefficient when parameters are adjusted by observations in section 4b. The most sensitive parameter is the damping coefficient O_d, which suggests that the viscosity and mixing coefficients of the ocean in a CGCM probably is the first candidate for parameter optimization. The second sensitive parameters are S_m and c_5 and the rest of 13 parameters stay in a similar level (Fig. 9b). The knowledge of the model sensitivities with respect to these model parameters will be used to determine the inflation amplitude of the prior ensemble of each parameter when the parameter is adjusted by observations in the next section.
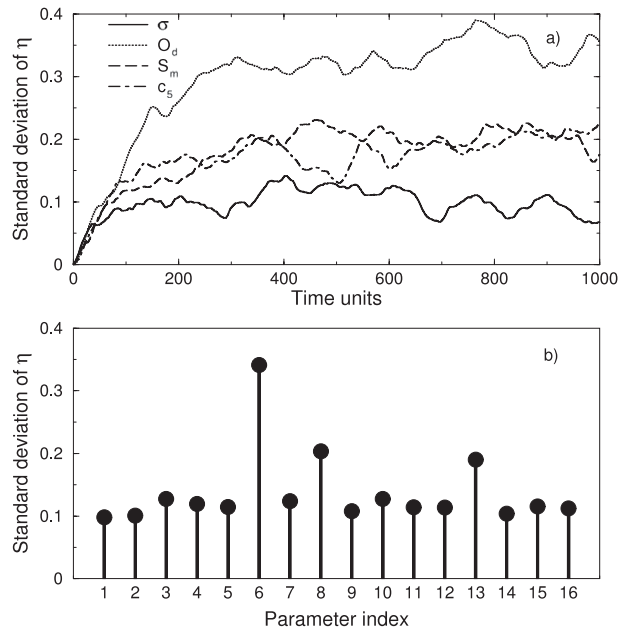
b. Optimization of model parameters

First, the time series of the normalized RMS of ensemble analysis increments by the model ensemble spread and the model climatological standard deviation is used to determine the time scale of the model ensemble in CDA being sufficiently constrained (Zhang et al. 2011). That is around 20 TUs in this simple model system, meaning that the process of CDA$_{\text{PO}}$ is activated after the CDA has gone through 200 steps of atmospheric assimilations (with 0.1 TU observational frequency) and 50 steps of oceanic assimilations (with 0.4 TU observational frequency). At each step of CDA$_{\text{PO}}$ (with the 0.1 TU interval) while all the coupled states are adjusted by the atmospheric and oceanic observations, all 16 parameters are also adjusted by the observations. The inflation scheme of the prior parameter ensemble in CDA$_{\text{PO}}$ is described as the following.

Usually, the inflation amplitude of a parameter ensemble is inversely proportional to the model sensitivity with respect to the parameter being estimated. So the inflation coefficient α_l in $\tilde{\beta}_l = \overline{\beta}_l + \alpha_l(\beta_l - \overline{\beta}_l)$ can be set as $\alpha_l = [1 + (\alpha_0\sigma_{l,0})/\sigma_l]$ where β_l represents the prior ensemble of the lth parameter, $\overline{\beta}_l$ is its mean, and $\tilde{\beta}_l$ is the inflated version. Then, a few trial-and-error tests find
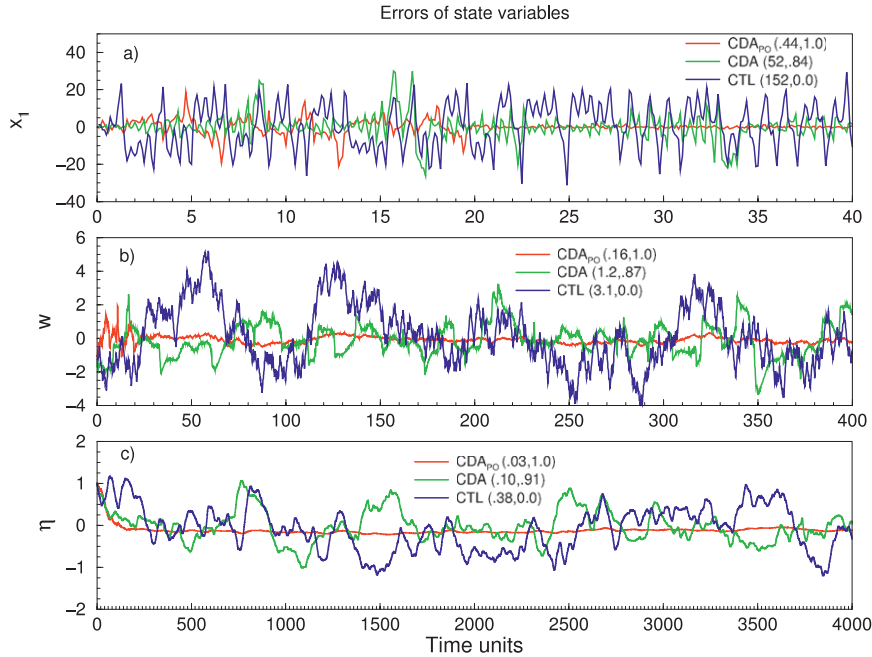
FIG. 10. Time series of the errors of the ensemble means of (a) x_1, (b) w, and (c) η produced by CDA$_{PO}$ (red) in which the parameter correction is activated at the 20th TU and traditional CDA (green). The free model ensemble CTL for which the assimilation model starts from the same ensemble initial conditions as CDA and CDA$_{PO}$ but without any data constraint is also plotted in blue in each panel as a reference. The pair of the numbers in the parenthesis for each line is the corresponding root-mean-square error (RMSE) and ACC verified with the truth.

$\alpha_0 = 10^{-3}$. This means that the prior ensemble of a parameter is enlarged to $10^{-3}/\sigma_l$ times of its initially guessed standard deviation $\sigma_{l,0}$ if the prior ensemble spread is smaller than this amount.

The errors of the ensemble means of typical atmospheric and oceanic state variables and all parameters varying with the times of CDA$_{PO}$ are shown in Figs. 10 and 11, respectively, in which the parameters are grouped according to their relative amplitudes of varying in different panels in Fig. 11. Figure 10 clearly shows that the CDA$_{PO}$ process adjusts both model states and parameters efficiently and constrains model uncertainties more dramatically than the CDA, evidenced by the diminishingly smaller oceanic errors and atmospheric errors compared to the CDA errors (reduced by 85%, see also Table 2).

Because of the compensative effect among all parameters and state variables in an ensemble filter (Yang and DelSole 2009), the optimization of parameters—expressed as a multivariate regression process of observational increments as formulated as Eq. (3)—does not however necessarily mean that each parameter converges to its truth. In fact, the solution of parameter optimization is a synthetic product of available observations, model sensitivities with respect to parameters as well as

other model bias sources except for erroneously set parameters. In this case, although only the erroneous model parameters serve as the only source of model bias, due to different availability of atmospheric and oceanic observations and the dependence of the parameter optimization on the deep ocean sensitivity, the subset of parameters has a different behavior in the optimization. For example, four atmospheric parameters, σ, b (Fig. 11a), κ (Fig. 11b), and c_1 (Fig. 11c) converge to their truth values very quickly while not all 12 oceanic parameters do so. It turns out that while the initial errors of eight oceanic parameters O_m, S_m, S_{pd} (Fig. 11a), Γ (Fig. 11b), c_3, c_4, c_6 (Fig. 11c), and γ (Fig. 11d) are greatly reduced through the optimization, the errors of the other four oceanic parameters S_s, O_d, c_2, and c_5 are not significantly reduced, some of them being even increased (S_s, for instance).

c. Impact of optimized model parameters on climate predictions

In this section, to assess the role of optimizing model parameters using observations for long time-scale predictions, four new forecast experiments (see Table 1) are conducted. In particular, to represent the different combination of model initial conditions and parameters, here an F with a subscript that indicates the initial conditions
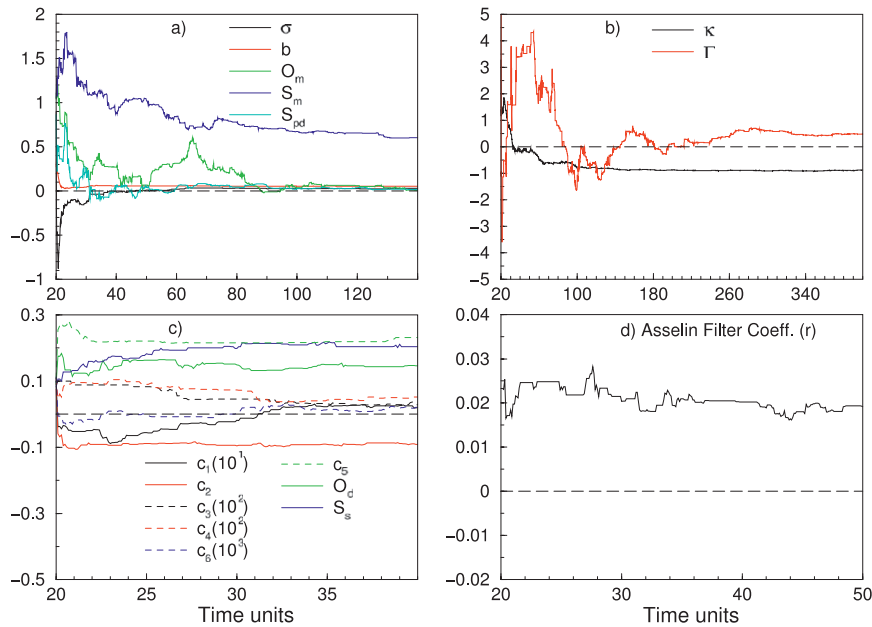
FIG. 11. Time series of the errors of the ensemble means of (a) σ, b, O_m, S_m, S_{pd}, (b) κ and Γ, (c) c_1, c_2, O_d, S_s, c_3, c_4, c_5 and c_6, and (d) γ optimized by the atmospheric observations at 0.1-TU frequency and the oceanic observations at 0.4-TU frequency. The horizontal black-dashed line in each panel marks the zero error (the truth).

and a superscript that indicates the used model parameters denotes a forecast experiment. For example, $F_{\mathrm{ICs(CDA_{PO})}}^{\mathrm{P(CDA_{PO})}}$ represents a forecast experiment in which both initial conditions and model parameters are produced by $\mathrm{CDA_{PO}}$ described in section 4.2. Another 3 forecast experiments are the following: $F_{\mathrm{ICs(CDA)}}^{\mathrm{P(CDA_{PO})}}$—with the CDA initial conditions but using the $\mathrm{CDA_{PO}}$-produced parameters, $F_{\mathrm{ICs(CDA_{PO})}}^{\mathrm{P(Truth)}}$—with the $\mathrm{CDA_{PO}}$ initial conditions but using the truth parameter, and $F_{\mathrm{ICs(Truth)}}^{\mathrm{P(CDA_{PO})}}$—with the perfect initial conditions taken from the truth but using $\mathrm{CDA_{PO}}$-produced parameters. The forecast ACCs and RMS errors produced by these four experiments are shown in Fig. 12 where the forecast skills produced by $F_{\mathrm{Ocn(CDA)}}^{\mathrm{Atm(CDA)}}$ are also marked by a black-dotted line in panels a, b, c as the reference to evaluate the impact of optimized model parameters. Again, $F_{\mathrm{Ocn(CDA)}}^{\mathrm{Atm(CDA)}}$ is a forecast experiment using CDA-produced coupled initial conditions without parameter optimization (its forecast ACC has been analyzed in section 3). The averaged ACCs and RMS errors of typical "weather" forecasts (x_1 in 2 TUs, for instance), SI (w in 5–15 TUs), and decadal (η in 50–150 TUs) predictions are shown in Fig. 13.

Compared to the traditional initialization scheme that only uses CDA to estimate model states ($F_{\mathrm{Ocn(CDA)}}^{\mathrm{Atm(CDA)}}$ dotted-black), the new initialization scheme using CDA to estimate both model states and parameters ($F_{\mathrm{ICs(CDA_{PO})}}^{\mathrm{P(CDA_{PO})}}$, red) greatly enhances the predictability of both the atmosphere and the ocean, evidenced by a much higher–lower

ACC–RMS error throughout the potential predictable period. If an ad hoc value of 0.6 ACC is used to characterize the time scale of a valid forecast/prediction (Hollingsworth et al. 1980), $\mathrm{CDA_{PO}}$ extends a valid forecast of the atmosphere by more than 5 times, (beyond 1.5 TUs from a quarter of TU). The valid prediction for the upper ocean is extended by 2 times, from a quarter of year to two thirds of year, while the predictability of the deep ocean is almost doubled, from a half decade to nearly one decade.

The different amplitude of predictability enhancement produced by $\mathrm{CDA_{PO}}$ for the atmosphere and the ocean is probably associated with the different roles of initial conditions and model parameters in atmospheric and oceanic predictions. The skills of both weather forecasts and climate predictions of $F_{\mathrm{ICs(CDA_{PO})}}^{\mathrm{P(CDA_{PO})}}$ (brown in Fig. 13) are better than the $F_{\mathrm{Ocn(CDA)}}^{\mathrm{Atm(CDA)}}$ (black in Fig. 13), suggesting that as the accuracy of initial conditions is lower, the forecast/prediction of a coupled model is not sensitive to the accuracy of model parameters. Except for the "weather" forecast (see Figs. 13a,d), both SI and decadal predictions of $F_{\mathrm{ICs(CDA)}}^{\mathrm{P(CDA_{PO})}}$ (red of Figs. 13b,c,e,f) are better than the $F_{\mathrm{ICs(Truth)}}^{\mathrm{P(CDA_{PO})}}$ (green of Figs. 13b,c,e,f) and the $F_{\mathrm{ICs(CDA_{PO})}}^{\mathrm{P(Truth)}}$ (blue of Figs. 13b,c,e,f). These comparisons address that, while initial conditions have stronger impacts on the "atmospheric" prediction, the coherence of optimized model parameters and initialized model states is critical to improve the long time-scale predictions.
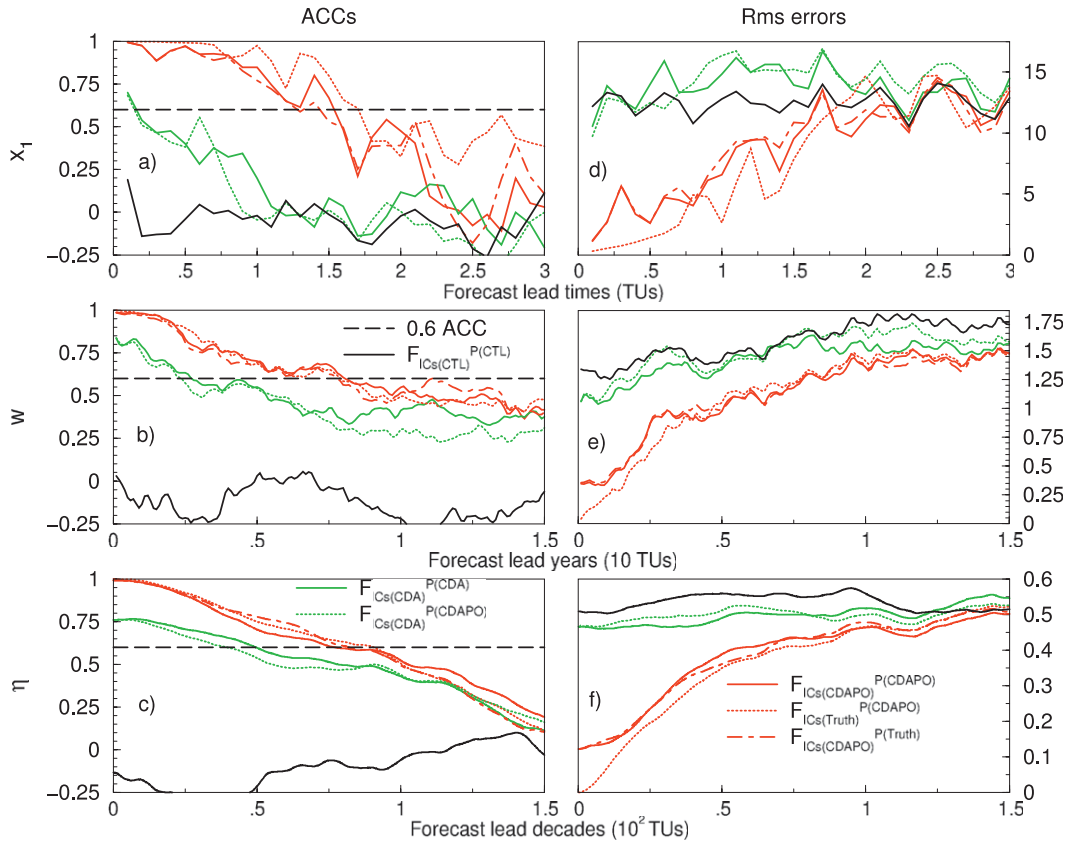
FIG. 12. Variations of the (a),(b),(c) ACCs and (d),(e),(f) normalized RMSEs by the climatological standard deviation of (a),(d) x_1, (b),(e) w, and (c),(f) η with the forecast lead time, produced by the CDA_{PO} initialization scheme ($F^{P(CDA_{PO})}_{ICs(CDA_{PO})}$, solid-red) and the traditional CDA initialization scheme ($F^{P(CDA)}_{ICs(CDA)}$, solid-green). $F^{P(CDA_{PO})}_{ICs(Truth)}$ (dotted-red), $F^{P(Truth)}_{ICs(CDA_{PO})}$ (dotted-dashed red), and $F^{P(CDA)}_{ICs(CDA)}$ (dotted-green) are used to detect the role of the coherence of optimized model parameters and initialized model states for climate predictions by replacing model parameters or initial conditions by a much more accurate version. The 0.6 ACC and 1 normalized RMS error are plotted by dashed-black lines as the benchmark of model predictability. The forecast ACCs produced by CTL (with no initialization), here called $F^{P(CTL)}_{ICs(CTL)}$, are plotted in (a),(b),(c) by solid-black lines as a reference to evaluate the forecast skill of an initialization scheme. Here, the climatological standard deviation is evaluated by $F^{P(CTL)}_{ICs(CTL)}$.

5. Conclusions and discussions

The erroneous values of parameters in a coupled model are a source of model bias that causes a climate prediction to drift away from the observed states (Smith et al. 2007). With the data assimilation scheme with enhancive parameter correction (Zhang et al. 2011), a simple pycnocline prediction model and a biased "twin" experiment framework are designed to study the impacts of observation-optimized coupled model states and parameters on various time scale climate predictions.

The simple pycnocline prediction model is based on Gnanadesikan's 2-term balance model that describes the zonal–time mean of pycnocline depth (Gnanadesikan 1999). The time tendency of the decadal anomalous pycnocline depth is derived as the residual of the low-latitude upwelling and the difference of the Northern Hemisphere sinking and the northward Ekman transport in the Southern Ocean, which is coupled with the upper-ocean variability. The coupling of the upper ocean and the atmosphere is represented by the four-variable conceptual coupled model in the previous study including the three Lorenz "chaotic" "atmospheric" variables and a slowly-varying "oceanic" variable representing "upper-ocean" variability. The simple model simulates a fundamental feature of a CGCM in which long time-scale variability of the deep ocean is driven by the upper ocean that is coupled with chaotic weather events. In the biased twin experiment, the assimilation model is set with a set of erroneous values for all model parameters while a "truth" model uses a set of standard parameter values. The "observations" are produced by sampling the truth using an "observing system" that simulates certain basic
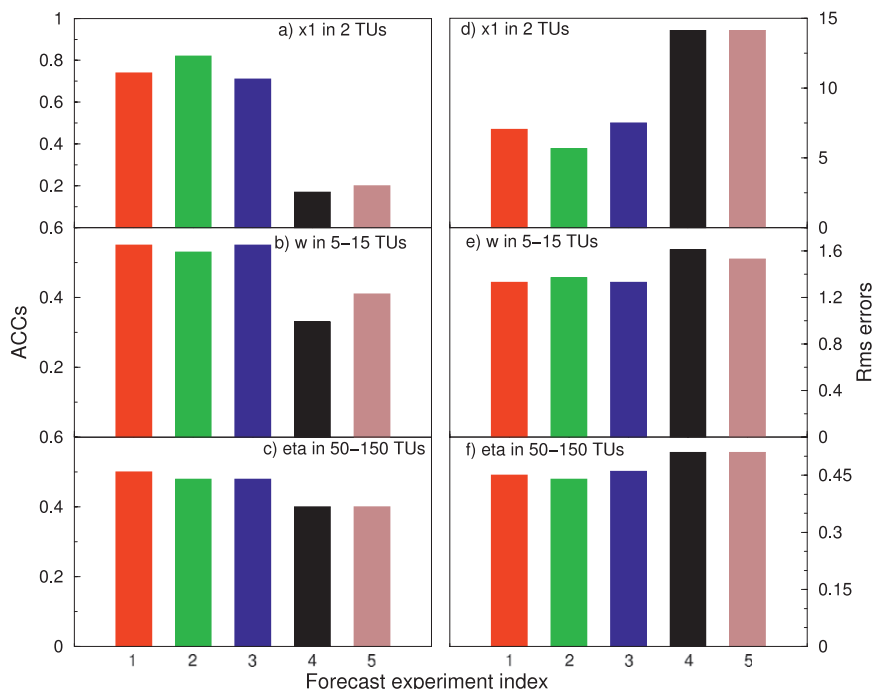
FIG. 13. The time-averaged (left) ACCs and (right) RMS errors of (a),(d) x_1 in the forecast lead time of 2 TUs, (b),(e) w in the forecast lead time of 5–15 TUs, and (c),(f) η in the forecast lead time of 50–150 TUs, produced by the forecast experiment $1-F_{\mathrm{ICs(CDA_{PO})}}^{\mathrm{P(CDA_{PO})}}$ (red), $2-F_{\mathrm{ICs(Truth)}}^{\mathrm{P(Truth)}}$ (green), $3-F_{\mathrm{ICs(CDA_{PO})}}^{\mathrm{P(CDA_{PO})}}$ (blue), $4-F_{\mathrm{ICs(CDA)}}^{\mathrm{P(CDA_{PO})}}$ (black), and $5-F_{\mathrm{Ocn(CDA)}}^{\mathrm{Atm(CDA)}}$ (brown).

features of the atmospheric and oceanic measurements in the real climate observing system. Then the synthetic atmospheric and oceanic observations are assimilated into the assimilation model to recover the truth, producing initial conditions and observation-optimized model parameters from which the model is initialized to predict the truth. The degree to which the predictions initialized from the estimated coupled model states from the traditional coupled data assimilation (e.g., Zhang et al. 2007) or the observation-optimized model states and parameters recover the truth is used to assess the impacts of the traditional coupled data assimilation and the coupled model state–parameter optimization scheme on the climate predictions of interests.

While the coupled model initialization through coupled data assimilation in which all coupled model components are coherently adjusted by observations minimizes the initial coupling shocks that reduce the forecast errors on seasonal-interannual time scales, the new initialization scheme that uses observations to optimize both coupled model states and parameters greatly enhances the predictability of the model on all time scales. For example, while the valid forecasts of the atmosphere are extended by more than 5 times, the predictability of the deep ocean is almost doubled. In addition, while the improved initial conditions from the new scheme have

stronger impacts on the atmospheric forecasts, the coherence of optimized model parameters and initialized model states is critical to improve the long time-scale predictions.

Although the coupled state–parameter optimization using observations has shown great promise with the simple pycnocline prediction model, serious challenges exist when it is applied to CGCMs to improve decadal predictions. First, in this simple model study, the errors of model parameters are the only source of model bias. In a CGCM, the misfittings from complex physical processes and dynamical core introduce multiple sources for model bias. The performance of the coupled state–parameter optimization scheme at the presence of multiple model biases needs to be examined further. Second, successful parameter optimization requires the good representation of an observing system and relies on the accuracy of estimated states. We may allow a parameter that traditionally takes a globally uniform value to vary geographically to reflect the geographical dependence of model sensitivity and observational availability. Given numerous parameters in a CGCM and the importance of model sensitivity knowledge in parameter optimization (Tong and Xue 2008a), a thorough sensitivity study of a CGCM with respect to its all parameters is a key but challenging first step. We may first start with

a few important (sensitive) parameters, which would have to be defined based on the modeler's knowledge about physical parameterizations. Theoretically, including parameters into assimilation control variables increases the freedom of an assimilation system so that the misfittings of climate modeling can be more efficiently constrained by observations thus reducing model biases. Once certain parameters that are sensitive for the processes of decadal variability [e.g. the North Atlantic overturning (Delworth et al. 1993) and the Pacific Rossby waves associated with the Pacific decadal oscillations (Schneider and Cornuelle 2005)] are identified and optimized, the improvement of decadal climate predictions through optimizing parameters of the CGCM holds promises.

REFERENCES

Aksoy, A., F. Zhang, and J. W. Nielsen-Gammon, 2006a: Ensemble-based simultaneous state and parameter estimation with MM5. *Geophys. Res. Lett.,* **33,** L12801, doi:10.1029/2006GL026186.

——, ——, and ——, 2006b: Ensemble-based simultaneous state and parameter estimation in a two-dimensional sea-breeze model. *Mon. Wea. Rev.,* **134,** 2951–2970.

Anderson, J. L., 2001: An ensemble adjustment Kalman filter for data assimilation. *Mon. Wea. Rev.,* **129,** 2884–2903.

——, 2003: A local least squares framework for ensemble filtering. *Mon. Wea. Rev.,* **131,** 634–642.

——, 2007: An adaptive covariance inflation error correction algorithm for ensemble filters. *Tellus,* **59A,** 210–224.

Annan, J. D., and J. C. Hargreaves, 2004: Efficient parameter estimation for a highly chaotic system. *Tellus,* **56A,** 520–526.

——, ——, N. R. Edwards, and R. Marsh, 2005: Parameter estimation in an intermediate complexity earth system model using an ensemble Kalman filter. *Ocean Modell.,* **8,** 135–154.

Asselin, R., 1972: Frequency filter for time integrations. *Mon. Wea. Rev.,* **100,** 487–490.

Cherupin, D., J. A. Carton, and D. Dee, 2005: Forecast model bias correction in ocean data assimilation. *Mon. Wea. Rev.,* **133,** 1328–1342.

Collins, W. D., M. L. Blackman, G. B. Bonan, J. J. Hack, T. B. Henderson, J. T. Kiehl, W. G. Large, and D. S. Mckenna, 2006: The Community Climate System Model version 3 (CCSM3). *J. Climate,* **19,** 2122–2143.

Dee, D. P., 2005: Bias and data assimilation. *Quart. J. Roy. Meteor. Soc.,* **131,** 3323–3343.

——, and A. M. D. Silva, 1998: Data assimilation in the presence of forecast bias. *Quart. J. Roy. Meteor. Soc.,* **124,** 269–295.

DelSole, T., and X. Yang, 2010: State and parameter estimation in stochastic dynamical models. *Physica D,* **239,** 1781–1788.

Delworth, T. L., S. Manabe, and R. J. Stouffer, 1993: Interdecadal variations of the thermohaline circulation in a coupled ocean-atmosphere model. *J. Climate,* **6,** 1993–2011.

——, and Coauthors, 2006: GFDL's CM2 global coupled climate models. Part I: Formulation and simulation characteristics. *J. Climate,* **19,** 643–674.

Evensen, G., 1994: Sequential data assimilation with a nonlinear quasi-geostrophic model using Monte Carlo methods to forecast error statistics. *J. Geophys. Res.,* **99,** 10 143–10 162.

——, 2007: *Data Assimilation: The Ensemble Kalman Filter.* Springer Press, 279 pp.

Gnanadesikan, A., 1999: A simple predictive model for the structure of the oceanic pycnocline. *Science,* **283,** 2077–2079.

Hamill, T. M., J. S. Whitaker, and C. Snyder, 2001: Distance-dependent filtering of background error covariance estimates in an ensemble Kalman filter. *Mon. Wea. Rev.,* **129,** 2776–2790.

Hansen, J., and C. Penland, 2007: On stochastic parameter estimation using data assimilation. *Physica D,* **230,** 88–89.

Hollingsworth, A., K. Arpe, M. Tiedtke, M. Capaldo, and H. Savijarvi, 1980: The performance of a medium-range forecast model in winter—Impact of physical parameterizations. *Mon. Wea. Rev.,* **108,** 1736–1773.

Keenlyside, N. S., M. Latif, J. Jungclaus, L. Kornblueh, and E. Roeckner, 2008: Advancing decadal-scale climate prediction in the North Atlantic sector. *Nature,* **453,** 84–88.

Kondrashov, D., C. Sun, and M. Ghil, 2008: Data assimilation for a coupled ocean-atmosphere model. Part II: Parameter estimation. *Mon. Wea. Rev.,* **136,** 5062–5076.

Lorenz, E. N., 1963: Deterministic non-periodic flow. *J. Atmos. Sci.,* **20,** 130–141.

Robert, A., 1969: The integration of a spectral model of the atmosphere by the implicit method. *Proc. WMO/IUGG Symp. on NWP,* Tokyo, Japan, Japan Meteorological Society, 19–24.

Schneider, N., and B. D. Cornuelle, 2005: The forcing of the Pacific decadal oscillation. *J. Climate,* **18,** 4355–4373.

Smith, D. M., S. Cusack, A. W. Colman, C. K. Folland, G. R. Harris, and J. M. Murphy, 2007: Improved surface temperature prediction for the coming decade from a global climate model. *Science,* **317,** 796–799.

Tong, M., and M. Xue, 2008a: Simultaneous estimation of microphysical parameters and atmospheric state with simulated radar data and ensemble square root Kalman filter. Part I: Sensitivity analysis and parameter identifiability. *Mon. Wea. Rev.,* **136,** 1630–1648.

——, and ——, 2008b: Simultaneous estimation of microphysical parameters and atmospheric state with simulated radar data and ensemble square root Kalman filter. Part II: Parameter estimation experiments. *Mon. Wea. Rev.,* **136,** 1649–1668.

Yang, X., and T. DelSole, 2009: Using the ensemble Kalman Filter to estimate multiplicative model parameters. *Tellus,* **61A,** 601–609.

Zhang, S., 2011: Impact of observation-optimized model parameters on decadal predictions: Simulation with a simple pycnocline

prediction model. *Geophys. Res. Lett.,* **38,** L02702, doi:10.1029/2010GL046133.

——, and J. L. Anderson, 2003: Impact of spatially and temporally varying estimates of error covariance on assimilation in a simple atmospheric model. *Tellus,* **55A,** 126–147.

——, and A. Rosati, 2010: An inflated ensemble filter for ocean data assimilation with a biased coupled GCM. *Mon. Wea. Rev.,* **138,** 3905–3931.

——, J. L. Anderson, A. Rosati, M. J. Harrison, S. P. Khare, and A. Wittenberg, 2004: Multiple time level adjustment for data assimilation. *Tellus,* **56A,** 2–15.

——, M. J. Harrison, A. Rosati, and A. T. Wittenberg, 2007: System design and evaluation of coupled ensemble data assimilation for global oceanic climate studies. *Mon. Wea. Rev.,* **135,** 3541–3564.

——, ——, and M. J. Harrison, 2009: Detection of multidecadal oceanic variability by ocean data assimilation in the context of a "perfect" coupled model. *J. Geophys. Res.,* **114,** C12018, doi:10.1029/2008JC005261.

——, Z. Liu, A. Rosati, and T. Delworth, 2011: A study of enhancive parameter correction with coupled data assimilation for climate estimation and prediction using a simple coupled model. *Tellus A,* in press.